Suppression of hydride precipitates in niobium superconducting radio-frequency cavities

Denise C Ford,[1,2] Lance D Cooley,[2] David N Seidman[3,4]

[1]Department of Chemical and Biological Engineering, Northwestern University, 2145 Sheridan Road, Evanston, IL 60208 USA
[2]Superconducting Materials Department, Technical Division, Fermi National Accelerator Laboratory, Batavia, IL 60510 USA
[3]Department of Materials Science and Engineering, Northwestern University, Evanston, IL 60208 USA
[4]Northwestern University Center for Atom-Probe Tomography (NUCAPT), Northwestern University, Evanston, IL 60208 USA

Email: deniseford@u.northwestern.edu

Abstract. Niobium hydride is a suspected contributor to degraded niobium superconducting radio-frequency (SRF) cavity performance by Q slope and Q disease. The concentration and distribution of hydrogen atoms in niobium can be strongly affected by the cavity processing treatments. This study provides guidance for cavity processing based on density functional theory calculations of the properties of common processing impurity species – hydrogen, oxygen, nitrogen, and carbon – in the body-centered cubic (bcc) niobium lattice. We demonstrate that some fundamental properties are shared between the impurity atoms, such as anionic character in niobium. The strain field produced, however, by hydrogen atoms is both geometrically different and substantially weaker than the strain field produced by the other impurities. We focus on the interaction between oxygen and hydrogen atoms in the lattice, and demonstrate that the elastic interactions between these species and the bcc niobium lattice cause trapping of hydrogen and oxygen atoms by bcc niobium lattice vacancies. We also show that the attraction of oxygen to a lattice vacancy is substantially stronger than the attraction of hydrogen to the vacancy. Additionally hydrogen dissolved in niobium tetrahedral interstitial sites can be trapped by oxygen, nitrogen, and possibly carbon atoms dissolved in octahedral interstitial sites. These results indicate that the concentration of oxygen in the bcc lattice can have a strong impact on the ability of hydrogen to form detrimental phases. Based on our results and a literature survey, we propose a mechanism for the success of the low-temperature annealing step applied to niobium SRF cavities. We also recommend further examination of nitrogen and carbon in bcc niobium, and particularly the role that nitrogen can play in preventing detrimental hydride phase formation.

Operated by Fermi Research Alliance, LLC under Contract No. De-AC02-07CH11359 with the United States Department of Energy.

1. Introduction

Superconducting radio-frequency (SRF) cavities fabricated from pure body-centered cubic (bcc) niobium are central components of high-energy and high-intensity particle accelerators. The SRF cavities undergo an intricate processing regimen to maximize the cavity quality factor, Q, and the accelerating gradient, during which multiple chemical polishing and high vacuum annealing steps are coordinated. Typically the regimen includes plastic forming of the cavity, heavy chemical polishing, high vacuum annealing at 600 or 800 °C and < 10^{-6} torr (hereafter called the high-temperature anneal), final chemical polishing, and final high vacuum annealing at 120 – 160 °C and < 10^{-6} torr (hereafter called the low-temperature anneal). Since the RF properties are determined over a few magnetic penetrations depths, of order 100 nm at 2 K, the regimen employed produces an empirical optimization of the near-surface nanostructure and nanocomposition.

The sensitivity of superconductivity and SRF cavity performance to near-surface details has invoked a tremendous materials science and engineering investigation. It was clear over 40 years ago [1] that the chemical polishing of a niobium surface results in a complicated interplay between hydrogen uptake, surface topographical features, and other trace atomic contaminants, such as oxygen, nitrogen, and carbon atoms [2]. The effect of these atomic contaminants, and in particular hydride precipitates, on niobium superconductivity has been demonstrated [3-9]; and numerous reports, see the review by Knobloch [10], describe how SRF cavities tested immediately after heavy chemical polishing developed a rapid drop of Q starting with zero accelerating gradient, a phenomena called "Q disease". Knobloch explains that a comparison of the phase diagrams, concentrations, diffusivities, and ability to enter or exit niobium during processing of these common processing impurities and cavity cool down rate versus performance statistics led to the belief that hydrogen is responsible for Q disease. Quantitative evaluation of hydrogen in SRF cavities has been, however, difficult; and in situ observations have not been possible. Even direct observations of precipitates in coupons and cavity cut-outs via scanning electron microscopy and transmission electron microscopy have only recently been presented [11]. Nevertheless, hydrogen is observed by residual gas analysis during the high-temperature anneal, correlating with improved cavity performance, thereby supporting the connection between hydrogen and Q disease.

The state of hydrogen in SRF cavities after the high-temperature anneal is still unclear, however. Hydrogen is present in the top 50 nm of the cavity near-surface region at greater concentrations than the equilibrium solubility, as demonstrated by recoil spectroscopy measurements [12, 13], atom-probe tomography measurements [14, 15], nuclear reaction analyses [16], and secondary ion mass spectrometry (SIMS) [17]. A light chemical polishing (removal of 20 μm) of the surface is typically performed after the high-temperature anneal, which may reintroduce some hydrogen into the cavity [18]. This hydrogen can then become trapped inside of the cavity because an oxide layer grows on the niobium upon exposure to water or air, which hinders the transport of hydrogen in or out of the niobium [9]. The enhanced concentration of hydrogen in the near-surface region may be due to trapping of dissolved hydrogen atoms by niobium lattice imperfections – such as vacancies, dislocations, or grain boundaries – other dissolved impurity atoms such as the oxygen provided by the oxide coating, or the interface between the oxide and niobium [19-21].

Many SRF cavities are operated immediately following the high-temperature anneal because only a small decrease of Q is observed with increasing RF field, often remaining above 10^{10} at surface RF magnetic fields up to ~100 mT. Above these fields, another phenomena called Q drop or high-field Q slope typically plagues cavities, and experiments utilizing arrays of thermometers on

the outside surface of a cavity demonstrate that eventually local sources of dissipation arise, resulting in the decrease of Q [22]. The cause of Q drop is currently unknown, however, the condition is often mitigated by the low-temperature anneal. Consequently, the underlying mechanisms for this effect are also not well understood, although a number of models have been proposed [17]. Recent studies suggest connections to the oxygen and hydrogen concentrations, and niobium vacancies, which we have shown to nucleate hydride precipitates in a recent density functional theory study [23]. However, a single model that explains all these effects does not exist. The active elements are:

- **Oxygen** – Surface x-ray techniques [24-26] have demonstrated that a low-temperature anneal (120-160 °C) changes the composition of the surface niobium oxides from mostly Nb_2O_5 to lower oxides and enhanced concentrations of interstitial oxygen atoms. Measurements of oxygen diffusion in niobium yield a diffusion length of ~40-200 nm in 48 h in this temperature range [27]. Therefore, an oxygen diffusion model has been proposed [28], which explains that during the low-temperature anneal, oxygen diffuses away from the niobium surface so that it can no longer affect cavity performance. Casalbuoni et al. [29], alternatively showed that low-temperature annealing increases the surface critical fields, consistent with the diffusion of oxygen into the near-surface region with a concomitant increase of electron scattering. Superconducting tunnel-junction measurements suggested a role is played by magnetic point defects created by vacant oxygen sites in the surface oxide [30, 31]; we are also studying this with first-principles computational techniques. Experiments that compared cavity properties before and after baking could not, however, elucidate any direct role of oxygen contamination or changes in the surface oxide for the mitigation of Q drop [17].

- **Hydrogen** – Visentin et al. [32] observed a correlation between positron annihilation – Doppler broadening parameters and a 145 °C anneal, which they attributed to release of hydrogen atoms from niobium vacancies. Romanenko [33] observed a reduction in the dislocation density after a 100-120 °C anneal, which he also attributed to the release of hydrogen from niobium vacancies resulting in an increased number of vacancies available to assist dislocation climb.

Motivated by these issues, we performed a first-principles density functional theory (DFT) based study of hydrogen and oxygen atoms in niobium, which we present in this article. We calculated the electronic and geometric properties of the impurity atoms dissolved in the interstices of the bcc niobium lattice as well as near niobium lattice vacancies. We also touched upon the properties of nitrogen and carbon in niobium. We discuss these results in terms of the formation of niobium hydride precipitates, and explain their implications for SRF cavity processing.

2. Methods

All calculations were performed with the Vienna Ab initio Simulation Package (VASP) [34, 35], using density functional theory (DFT), periodic boundary conditions, and a plane wave basis set with a 400 eV kinetic energy cutoff. The generalized gradient approximation (GGA) was used with the Perdew, Burke, Ernzerhof (PBE) exchange-correlation functional [36], and the core electrons were described by the projector-augmented-wave (PAW) pseudopotentials [37, 38]. All of the structure optimizations were calculated with all of the atom and cell degrees of freedom relaxed. Forces were converged to 0.02 eV/Å. The geometry was optimized for each crystal structure with a 2x2x2 gamma-centered Monkhorst-Pack [39] k-point mesh. The partial occupancies for the wavefunctions were set by the 1st order Methfessel-Paxton method with a smearing width of 0.2 eV. The Bader method was used to assign charges to individual atoms [40-42].

The properties of the interstitial impurities H, O, N, and C in bcc niobium were assessed in 4x4x4 unit cells (128 atoms). The unit cell was chosen to be computationally efficient while minimizing interactions between the periodic images. It is not intended to represent a specific concentration of defects. Several tests were performed for larger unit cells and the conclusions drawn in this paper were upheld. The calculated Nb lattice parameter without impurity atoms is 3.32 Å, which is in good agreement with the experimental lattice constant of 3.30 Å [43]. Tetrahedral and octahedral interstices were considered as absorption sites for these impurity species. This unit cell was also used to assess the interactions between hydrogen and oxygen atoms, and a niobium lattice vacancy. The vacancy was created by removing one Nb atom, which corresponds to a vacancy concentration of 0.8 at.%. The calculated vacancy formation energy is 2.71 eV, which is in good agreement with the experimentally determined range 2.6-3.1 eV given in a review by Schultz and Ehrhart [44] and other first-principles calculations [45, 46].

Several energetic properties are discussed in the results section for comparison between structures. Binding energies were calculated from various reference states as were appropriate for the discussion, and these are specified in the results section. Negative (-) binding energies indicate that the bound state is lower in energy than the unbound state. Strain energies were calculated as the difference between the ideal bcc niobium lattice and the lattice expanded by an impurity atom. Zero-point vibrational energy (ZPE) is included in all of the energy calculations, and was calculated from the formula $E = 0.5h\Sigma\nu_i$, where h is Planck's constant and ν_i are the frequencies of the vibrational modes. The vibrational frequencies were determined from the Hessian matrix, which was created via a finite differences approach with a step size of 0.015 Å. Since large supercells were used (at least 127 atoms), only the vibrations of the impurity atoms were considered (i.e. the differences between the vibrational energies of the niobium atoms in each calculation was assumed to be negligible). For example, the ZPE associated with the migration of a hydrogen atom from an interstitial absorption site in bcc niobium to an absorption site in a niobium lattice vacancy was calculated as ZPE($Nb_{127}H$, H only relaxed) – ZPE($Nb_{128}H$, H only relaxed).

3. Results and Discussion

3.1 Interstitial hydrogen, oxygen, nitrogen, and carbon atoms

Dissolved oxygen, nitrogen, and carbon are all found in SRF niobium [47], and all occupy octahedral lattice interstitial sites. Specifications for niobium restrict the concentrations of these interstitial elements to <30 mass ppm (<200 atomic ppm) [48]. The charge acquired by these interstitial impurity atoms when absorbed into bcc niobium is 2-3 times greater than the charge acquired by interstitial hydrogen atoms; and their binding energies, referred to the impurity atoms in the gas phase, is about 2.5-3.5 times greater than that of hydrogen (table 1). The atomic radii of these impurity atoms and their bond lengths are given in table 2, which shows that the diameters of O, N, and C are at least 0.78 Å larger than the shortest distance between niobium atoms surrounding an octahedral site, and at least 0.40 Å smaller than the longest distance between niobium atoms surrounding an octahedral site. Thus, an anisotropic lattice deformation consisting of an increase in the short distance between niobium atoms and a decrease in the long distance between niobium atoms surrounding an octahedral site occurs when an octahedral site absorbs an oxygen, nitrogen or carbon atom. We have previously shown that hydrogen occupies tetrahedral lattice interstitial sites in bcc niobium [23], and its atomic radius is comparable to the size of a tetrahedral site; thus a much smaller lattice deformation occurs upon the absorption of hydrogen into the niobium lattice interstices. Additionally, all four of the bonded niobium atoms are pushed outwards upon absorption of a hydrogen atom into the interstice. The geometries of tetrahedral and octahedral sites are depicted in figure 1. Since interstitial oxygen is present in

large and variable quantities in SRF niobium due to oxidation of the surface and contact with water, and the properties of nitrogen, carbon, and oxygen interstitials are similar, the effects of oxygen on hydrogen absorption and phase formation is the focus of the remainder of this study.

Table 1. Charges on the niobium atoms bonded to the interstitial impurity atoms – H, O, N and C – and on the interstitial impurities; binding energies of the interstitial impurities absorbed into a bcc niobium lattice interstitial site referred to bcc niobium and the impurity species as an atom in the gas phase; and the lattice strain energies caused by the impurity species residing in the interstice. H occupies tetrahedral binding sites; and O, N, and C occupy octahedral binding sites. The charge for Nb atoms with 'b' bonds to the impurity atoms is given first in the table and for Nb atoms with 'c' bonds is given second. See figure 1 for an illustration of the binding geometries.

	Nb_{128}	$Nb_{128}H$	$Nb_{128}O$	$Nb_{128}N$	$Nb_{128}C$
Charge on bonded Nb (e)	-0.01/0.01	0.14	0.12/0.23	0.21/0.31	0.26/0.37
Charge on interstitial atom (e)	-	-0.65	-1.35	-1.63	-1.76
Binding energy (eV)	-	-2.41	-7.02	-7.39	-8.48
Lattice strain energy (eV)	-	0.11	0.83	0.83	0.96

Table 2. Nb-interstitial impurity bond lengths. Tetrahedral (tet.) sites provide four equidistant bonds, 'a' and octahedral (oct.) sites provide two *equidistant short bonds*, 'b', and four *equidistant long bonds*, 'c'. An n/a table entry means not applicable. The geometries are depicted in figure 1.

	Impurity–Nb Bond Length (Å)			Atomic Radius
	a	b	c	(Å)[49]
Nb128 tet. site*	1.86	n/a	n/a	1.45 (Nb)
Nb128H	1.94	n/a	n/a	0.25 (H)
Nb128 oct. site*	n/a	1.66	2.35	1.45 (Nb)
Nb128O	n/a	2.04	2.30	0.60 (O)
Nb128N	n/a	2.05	2.24	0.65 (N)
Nb128C	n/a	2.08	2.24	0.70 (C)

* hypothetical bond lengths in the lattice sites that are not deformed by impurity absorption.

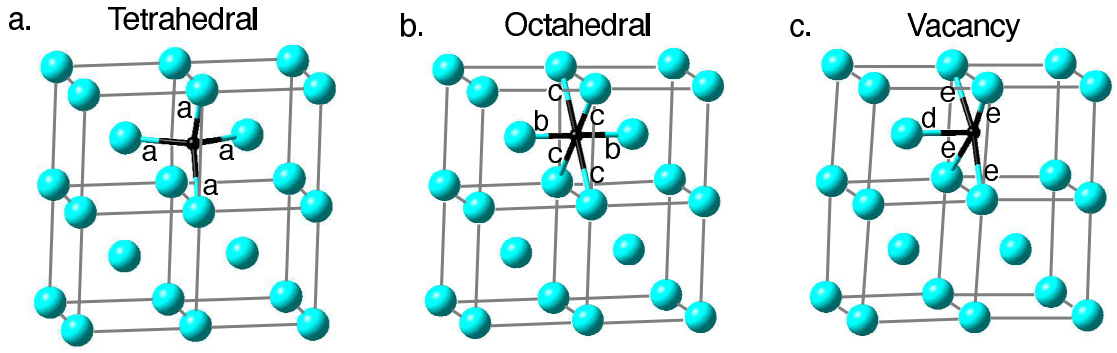

Figure 1. Illustration of (a) tetrahedral, (b) octahedral, and (c) vacancy binding sites in bcc niobium. A small black sphere represents an impurity atom and large light-blue spheres represent niobium atoms. The niobium-impurity atom bonds labeled 'a' are equidistant, niobium-impurity atom bonds labeled 'b' are equidistant, etc. The bond lengths are given in tables 2 and 5.

3.2 Hydrogen trapping by other interstitial impurities

Dissolved hydrogen atoms can become trapped by several mechanisms, including other interstitially dissolved impurity atoms. Prior studies have demonstrated that a dissolved oxygen or nitrogen atom can bind one hydrogen atom in a nearby absorption site with a binding energy, referred to a hydrogen atom dissolved in a bcc niobium tetrahedral interstice infinitely far away from the trapping impurity, of approximately -0.1 eV [50-53]. The trapping effect has been explained by an expansion of the some of the nearby interstitial absorption sites resulting from the lattice deformation caused by the absorption of the other impurity atom into an octahedral site. The ideal trapping site is both close enough to the other impurity to benefit from the elastic expansion of the lattice, yet sufficiently far away to minimize the Coulomb repulsion between the two impurity atoms. Several theoretical [52, 54] and experimental [55-59] studies have been performed to identify the trapping configuration, but there still remains controversy.

Occupancy of tetrahedral sites by trapped hydrogen atoms has been established by neutron spectroscopy [59], although the site is not equivalent to a tetrahedral site that is not in the vicinity of the trapping impurity. The non-equivalency has been demonstrated by ion channeling experiments with a nuclear reaction [58], where the authors propose occupation of displaced tetrahedral sites. Additionally x-ray scattering experiments [57] demonstrate a change in symmetry from cubic for free interstitial hydrogen to tetragonal for trapped hydrogen. We have shown in Section 3.1 that the bcc niobium lattice is distorted substantially in the neighborhood of an absorbed oxygen or nitrogen atom.

We determined the O-H trapping configuration by calculating the binding energy for a hydrogen atom in absorption sites up to 8.5 Å away from an oxygen atom in an octahedral site. All of our initial configurations included hydrogen atoms in tetrahedral sites; however, the coordinates of all of the atoms were relaxed during the geometry optimization calculations, so the hydrogen atom would have been free to move into nearby octahedral, trigonal, etc. sites. We find that the only significantly favorable (binding energy of -0.06 eV) site is a tetrahedral site in-plane with the four long Nb-O bonds; this site provides one bond to one of these niobium atoms and three bonds to niobium atoms that are not bonded to the oxygen atom, figure 2. The configuration represents a 6^{th} nearest-neighbor pair with an O-H distance of 4.11 Å. The bond lengths between the four niobium atoms and the hydrogen atom are not exactly equivalent in our suggested configuration, with the hydrogen atom being displaced slightly toward the oxygen atom. The differences in the Nb-H bond lengths are ~0.04 Å. In agreement with [59], we only find small differences in the energies of hydrogen's three vibrational modes (two occur at the same energy) between the trapped and free states: -2 and 7 meV. We also find only small differences in charges between the trapped and free states: +0.02 e on the oxygen atom and -0.02 e on the hydrogen atom.

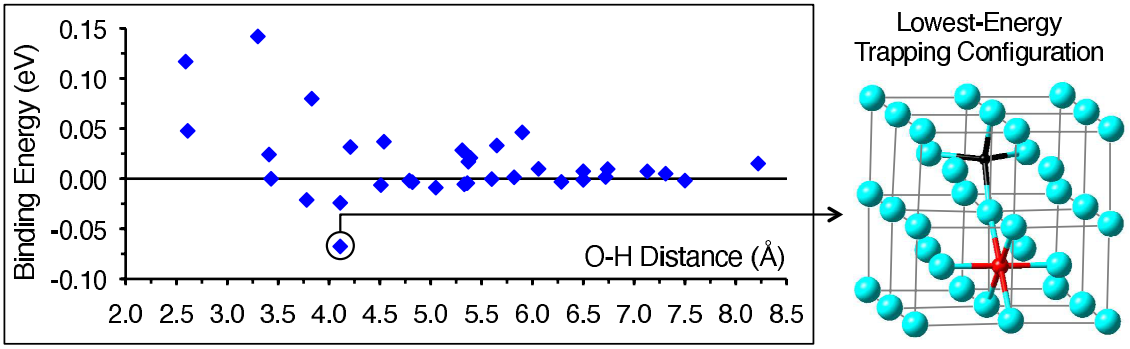

Figure 2. Plot of binding energy, referred to a hydrogen atom in a bcc niobium tetrahedral interstice and an oxygen atom in an infinitely far away octahedral interstice, versus the distance between an oxygen atom in an octahedral interstice and a trapped hydrogen atom in a nearby tetrahedral interstice. The highest-energy configuration is not shown on the plot because it is substantially higher in energy than all of the other configurations; its coordinates are (2.17, 0.36). ZPE was neglected in these binding energy calculations, but the contribution was checked for the lowest-energy configuration and found to be ~0.005 eV. A diagram of the lowest-energy configuration is also shown. Niobium atoms are represented by large light-blue spheres, the oxygen atom by a medium red sphere, and the hydrogen atom by a small black sphere.

We also calculated the trapping energy for the lowest-energy O-H trapping configuration while replacing the oxygen atom with a nitrogen atom, -0.10 eV. The similar but slightly larger binding energy for a nitrogen atom compared to an oxygen atom is in agreement with experiments [50, 51, 53], and consistent with our report of the lattice deformation being similar but larger in magnitude for a nitrogen atom compared to an oxygen atom (table 2).

Finally, it may be possible for each oxygen or nitrogen atom to trap more than one hydrogen atom when a niobium specimen is cooled rapidly [60, 61]. The site occupied by a hydrogen atom in our lowest-energy trapping configuration exists in eight symmetrically equivalent sites around the oxygen atom, and four of these sites are available for the simultaneous occupation of different hydrogen atoms. A kinetic study is, however, required to shed further light on the trapping of multiple hydrogen atoms by a single oxygen or nitrogen atom, which is outside of the scope of this study.

3.3 Hydrogen and oxygen trapping by niobium lattice vacancies

The charge distribution, and binding and lattice strain energies (referred to the appropriate number of hydrogen atoms in bcc niobium tetrahedral interstices and oxygen atoms in octahedral interstices) caused by different numbers of hydrogen and oxygen atoms residing in a niobium lattice vacancy are listed in table 4. Both hydrogen and oxygen occupy the same type of vacancy binding site, which is similar to an octahedral binding site, less one niobium atom that would form a short bond (figure 1 and table 5). In a previous study where we considered only hydrogen atoms [23], we found that six hydrogen atoms occupying the six symmetrically equivalent octahedral-like sites was the most stable configuration, and was strongly preferred to hydrogen atoms occupying the tetrahedral lattice interstices. In this study, we find that that the binding energy to a vacancy is twice as large for an oxygen atom as it is for a hydrogen atom, and a niobium lattice vacancy can bind a maximum of four oxygen atoms. The calculated binding energies of -0.79 eV for an oxygen atom and -0.41 eV for a hydrogen atom are in good agreement with values obtained from experiments [62, 63].

Table 4. Charges on niobium atoms bonded to an impurity atom and on the impurity atoms; and binding and lattice strain energies of the impurity atoms in niobium lattice sites and vacancies referred to the isolated impurity atoms located in their preferred interstitial sites. Where two table entries are present, the first one applies to a niobium atom in a type 'b' or 'd' bond and the second entry applies to a niobium atom in a type 'c' or 'e' bond. See figure 1 for the definition of bond types.

	Nb_{128}	$Nb_{128}H$	Nb_{127}	$Nb_{127}H$	$Nb_{127}H_4$	$Nb_{127}H_6$
Charge on bonded Nb (e)	-0.01/0.01	0.14	0.08	0.11/0.13	0.08/0.26	0.11/0.32
Charge on H (e)	-	-0.65	-	-0.56	-0.53	-0.52
Binding energy per H (eV)	-	0.00	-	-0.41	-0.39	-0.34
Lattice strain energy per H (eV)	-	0.00	-	-0.09	-0.09	-0.09
	Nb_{128}	$Nb_{128}O$	Nb_{127}	$Nb_{127}O$	$Nb_{127}O_4$	$Nb_{127}O_6$
Charge on bonded Nb (e)	-0.01/0.01	0.12/0.23	0.08	0.09/0.29	0.20/0.54	0.22/0.74
Charge on O (e)	-	-1.35	-	-1.32	-1.28	-1.19
Binding energy per O (eV)	-	0.00	-	-0.79	-0.24	0.20
Lattice strain energy per O (eV)	-	0.00	-	-0.59	-0.43	-0.31

Table 5. Nb-impurity bond lengths when an impurity atom is located in a niobium lattice vacancy. The geometry is similar to the octahedral binding geometry, figure 1, and consists of one *short bond,* 'd', and four *equidistant long bonds*, 'e'.

	Impurity – Nb Bond Length (Å)	
	d	e
Nb127H	1.97	2.27
Nb127O	2.14	2.19

A Bader analysis of the local charges shows that the addition of one oxygen atom to a vacancy causes only a 0.04 e decrease in the charge on an oxygen atom, and the bonding changes from four niobium atoms with a +0.23 e charge and two with a +0.12 e charge to four with a +0.29 e charge and one with a +0.09 e charge. Given the small change in the charge on an oxygen atom when residing in a vacancy, the decrease in binding energy can be attributed largely to the relaxation of the lattice strain. Addition of more oxygen atoms to a vacancy is favored, although the stability decreases for each additional oxygen atom. The charge on each oxygen atom also continues to decrease and the charges on the bonded niobium atoms continue to increase, which destabilizes these configurations. The lattice strain energy, however, is still less than what it would be if the oxygen atoms were residing in isolated octahedral interstices. Six oxygen atoms residing in one vacancy is less stable than dispersing them to six octahedral interstices. Although lattice strain energy is reduced for hydrogen migration from a tetrahedral binding site to a vacancy binding site, the magnitude is considerably less than for oxygen migration from an octahedral site to a vacancy site.

One hydrogen atom and one oxygen atom can occupy a single vacancy at about the same energy compared to when they are located in different vacancies. When the vacancy is, however, filled with four oxygen atoms, it becomes unfavorable for hydrogen atoms to fill the remaining two octahedral-like absorption sites. Furthermore, similar to the distribution shown in figure 2 for hydrogen atom trapping by an interstitial oxygen atom, many of the tetrahedral sites surrounding a vacancy occupied by oxygen atoms are blocked from occupation by hydrogen atoms. We found a similar trapping configuration for an oxygen atom in a vacancy binding site and a hydrogen atom in a tetrahedral lattice site as for an oxygen atom in an octahedral site and a hydrogen atom in a tetrahedral site with a similar trapping energy, -0.10 eV; therefore, oxygen atoms do not lose their ability to trap hydrogen atoms by occupying niobium lattice vacancies.

3.4 Implications for Superconducting Radio-Frequency Cavity Processing

Based on our results and a literature review, we suggest a mechanism for the success of the low-temperature anneal (120-160 °C): 1. Hydrogen atoms are released from the ordered niobium hydride phases and niobium vacancies, and they diffuse into the niobium bulk. 2. Oxygen atoms are released from the octahedral niobium interstitial sites and from the oxide layers, and then migrate into the vacancies within the first 100 nm subsurface region; this prevents hydride phases from precipitating around niobium defect nucleation sites in the subsurface region. 3. Hydrogen atoms become trapped by oxygen, nitrogen, and possibly carbon atoms dissolved in the niobium, so they cannot find each other to form the precipitated phases. The evidence is discussed in the following paragraphs.

The niobium-hydrogen phase diagram [64] indicates that there shouldn't be precipitated niobium hydride phases above 90 °C for a hydrogen concentration of up to ~34 at. %. Therefore, the low temperature anneal should be sufficient to dissociate any pre-existing ordered niobium hydride precipitate phases. The low temperature anneal should also be sufficient to dissociate vacancy-hydride clusters, since Hautojärvi et al. [65] demonstrated via positron–annihilation spectroscopy that this occurs at ~110 °C.

We have demonstrated that the binding energy of oxygen atoms to niobium vacancies is stronger than the binding energy of hydrogen atoms to vacancies, and researchers performing internal friction experiments have shown that oxygen atoms cannot escape from the vacancies below 200 °C [62]. It has also been shown via resistivity experiments that oxygen can migrate to and become trapped at lattice vacancies between 100-175 °C [66, 67]. Oxygen can be supplied to the vacancies by the oxide layers, as it has been shown via x-ray scattering experiments that the oxide phases begin to dissociate in the temperature range of the low-temperature anneal [24-26], or by interstitial oxygen atoms, as it has been determined via multiple experimental methods that oxygen atoms can diffuse at least 40 nm in niobium in this temperature range [27]. Thus, oxygen from the oxide layers or oxygen dissolved in niobium interstices may become mobile during the low temperature anneal, but get trapped in sinks such as niobium vacancies: this prevents the oxygen in the top 100 nm from diffusing far into the bulk, consistent with the results of the diffuse x-ray scattering experiments [25] which showed that the oxygen released from the oxide layers after a 5 h anneal at 145 °C remained within 10 nm of the oxide-niobium interface. Additionally, when the annealing temperature in [25] was increased to 300 °C the dissolved oxygen had diffused beyond the 10 nm probing depth of the grazing x-rays, consistent with oxygen becoming detrapped from vacancies, and by extension other lattice imperfections, above 200 °C.

The defect concentration of SRF niobium has recently been studied via positron annihilation – Doppler broadening [32]. The researches compared the results of a cavity annealed in air to a cavity annealed in argon for 3 h at 145 °C and did not think that the introduction of oxygen into the cavity from air annealing significantly affected the niobium vacancy concentration. However, the low momentum annihilation fraction (S), which is sensitive to the defect concentration, did exhibit a noticeable difference between these samples (albeit less significant than the difference between samples that were annealed compared to samples that were not annealed, which was interpreted as the detrapping of hydrogen from niobium vacancies during the anneal). Therefore, the migration of oxygen atoms into the vacancies may have occurred during this experiment, but the effect was not pronounced for the specific experimental conditions. Therefore, we suggest further studies into oxygen migration to niobium lattice vacancies at conditions relevant to SRF cavity processing. For example, it would be useful to perform an isothermal aging experiment at different temperatures between 120 and 160 °C on SRF niobium. Also, positron lifetime experiments may be able to elucidate the difference between oxygen occupied, hydrogen

occupied, and unoccupied niobium lattice vacancies. The results of our calculations demonstrate the rearrangement of electrons for these different situations, and the calculated wavefunctions of the atoms involved in these scenarios can aid in the interpretation of positron experiments.

We have also demonstrated that dissolved oxygen and nitrogen atoms can trap dissolved hydrogen atoms in the bcc niobium lattice; therefore, these impurities can inhibit significantly the kinetics for precipitation of niobium hydrides. We have also shown that dissolved carbon atoms have similar properties to dissolved oxygen and nitrogen atoms, so by extension, carbon can also participate in the prevention of niobium hydride precipitation. These results are consistent with observations of reactor grade niobium (residual resistivity ratio of 40) being less susceptible to Q-disease than high purity niobium (residual resistivity ratio of 500) [10].

Finally, experimental studies have demonstrated that nitrogen atoms require a higher temperature to both trap (~300 °C) and liberate (~500 °C) them from a niobium vacancy [62, 66]. Therefore, nitrogen could be used for more aggressive hydrogen sequestration. Furthermore, tetragonal and cubic niobium nitrides have superconducting transition temperatures > 10 K, so their formation would not be detrimental to cavity performance. Therefore, we suggest further research concerning nitrogen in niobium in the context of suppressing niobium hydride formation.

4. Summary

We performed a density functional theory study of the electronic and geometric properties of interstitial hydrogen, oxygen, nitrogen, and carbon atoms in niobium, and hydrogen and oxygen atoms in niobium site vacancies. We find that:

- Interstitial hydrogen atoms occupy tetrahedral sites in the bcc niobium lattice; whereas interstitial oxygen, nitrogen, and carbon atoms occupy octahedral sites. Hence, interstitial hydrogen atoms cause a different type of lattice deformation than the other interstitial impurity atoms.
- The niobium lattice strain energy is 0.72 eV less for the absorption of a hydrogen atom than for the absorption of an oxygen or a nitrogen atom, and 0.85 eV less than for the absorption of a carbon atom.
- Dissolved hydrogen atoms can become trapped by dissolved oxygen, nitrogen, and possibly carbon atoms.
- All of the interstitial impurity atoms have partially anionic character in the bcc niobium lattice. Therefore, their Coulomb interactions are repulsive and the trapping of hydrogen atoms by the other types of impurity atoms is due to the elastic deformation of the lattice in the neighborhood of the trapping atom.
- One niobium vacancy is able to absorb up to six hydrogen atoms or four oxygen atoms; however, the absorption of an oxygen atom by a lattice vacancy is 0.38 eV more favorable than the absorption of a hydrogen atom.
- The absorption of an oxygen atom into a niobium lattice vacancy does not prevent the oxygen atom from trapping a hydrogen atom.

We suggest that oxygen, nitrogen, carbon, and hydrogen atoms, and niobium lattice vacancies are all involved in the alleviation of Q drop resulting from the low-temperature (120 – 160 °C) anneal. We propose the following mechanism to explain the extant experimental observations:

- Hydrogen atoms are released from the ordered niobium hydride phases and niobium vacancies, and they diffuse into the niobium bulk.
- Oxygen atoms are released from the octahedral niobium interstitial sites and from the oxide layers, and then migrate into the vacancies in the niobium subsurface: this prevents

hydrogen atoms from returning to the vacancies that served as nucleation centers for hydride precipitates.

- Hydrogen atoms become trapped by oxygen, nitrogen, or possibly carbon atoms dissolved in the niobium, so they cannot find each other to form precipitated phases.

Finally, we suggest that nitrogen is further studied in the context of preventing niobium hydride precipitation.

Acknowledgements
Operated by Fermi Research Alliance, LLC under Contract No. De-AC02-07CH11359 with the United States Department of Energy.

References

[1] Hoyt E W 1972 Niobium surfaces for rf superconductors *J. Vac. Sci. Technol.* **9** 144-54
[2] Padamsee H 2009 *RF Superconductivity Science, Technology and Applications* vol II (Weinheim: Wiley-VCH)
[3] Jisrawi N M, Ruckman M W, Thurston T R, Reisfeld G, Weinert M, Strongin M and Gurvitch M 1998 Reversible depression in the Tc of thin Nb films due to enhanced hydrogen adsorption *Phys. Rev. B* **58** 6585-91
[4] Welter J-M and Johnen F J 1977 Superconducting transition temperature and low temperature resistivity in the niobium-hydrogen system *Z. Physik B* **27** 227-32
[5] Ohlendorf D and Wicke E 1979 Heat capacities between 1.5 and 16 K and superconductivity of V/H and Nb/H alloys *J. Phys. Chem. Solids* **40** 721-8
[6] DeSorbo W 1963 Effect of dissolved gases on some superconducting properties of niobium *Phys. Rev.* **132** 107
[7] Vinnikov L Y and Goluboe A O 1982 Direct observation of magnetic structure in niobium single crystals with hydride precipitate pinning centres *Phys. Stat. Sol.* **69** 631-6
[8] Welling M S, Aegerter C M, Westerwaal R J, Enache S, Wijngaarden R J and Griessen R 2004 Effect of hydrogen uptake and substrate orientation on the flux penetration in NbHx thin films *Physica C* **406** 100-6
[9] Isagawa S 1980 Hydrogen absorption and its effect on low-temperature electric properties of niobium *J. Appl. Phys.* **51** 4461-70
[10] Knobloch J 2003 The "Q disease" in superconducting niobium RF cavities. In: *Hydrogen in Materials & Vacuum Systems: First International Workshop on Hydrogen in Materials and Vacuum Systems,* ed G R Myneni and S Chattopadhyay (Melville, New York: AIP) pp 133-50
[11] Barkov F, Romanenko A and Grassellino A 2012 Direct observation of hydrides formation in cavity-grade niobium *Phys. Rev. ST Accel. Beams* **15** 122001
[12] Romanenko A and Goncharova L V 2011 Elastic recoil detection studies of near-surface hydrogen in cavity-grade niobium *Supercond. Sci. Tech.* **24** 105017
[13] Antoine C 1991 Hydrogen in niobium : the analytical approach. In: *Proc. of the 5th Workshop on RF superconductivity,* (DESY, Hambourg, Germany)
[14] Kim Y-J and Seidman D N Atom-scale analyses of Nb-hydrides via local-electrode atom-probe tomography **sumbitted**
[15] Kim Y-J and Seidman D N Atomic-scale chemical analyses of niobium-hydrides using atom-probe tomography and transmission electron microscopy **submitted**
[16] Ciovati G 2004 Effect of low-temperature baking on the radio-frequency properties of niobium superconducting cavities for particle accelerators *J. Appl. Phys.* **96** 1591-601
[17] Ciovati G, Myneni G, Stevie F, Maheshwari P and Griffis D 2010 High field Q slope and the baking effect: review of recent experimental results and new data on Nb heat treatments *Phys. Rev. ST Accel. Beams* **13** 022002

[18] Ricker R E and Myneni G R 2010 Evaluation of the propensity of niobium to absorb hydrogen during fabrication of superconducting radio frequency cavities for particle accelerators *J. Res. Natl. Inst. Stand. Technol.* **115** 353-71
[19] Myers S M, Baskes M I, Birnbaum H K, Corbett J W, DeLeo G G, Estreicher S K, Haller E E, Jena P, Johnson N M, Kirchheim R, Pearton S J and Stavola M J 1992 Hydrogen interactions with defects in crystalline solids *Rev. Mod. Phys.* **64** 559-617
[20] Khaldeev G V and Gogel V K 1987 Physical and corrosion-electrochemical properties of the niobium hydrogen system *Russ. Chem. Rev.* **56**
[21] Halbritter J 1987 On the oxidation and on the superconductivity of niobium *Appl. Phys. A* **43** 1-28
[22] Ciovati G 2006 Review of the frontier workshop and Q-slope results *Physica C* **441** 44-50
[23] Ford D C, Cooley L D and Seidman D N First-principles calculations of niobium hydride formation in superconducting radio-frequency cavities *Supercon. Sci. Technol.* **submitted**
[24] Ma Q, Ryan P, Freeland J W and Rosenberg R A 2004 Thermal effect on the oxides on Nb(100) studied by synchrotron-radiation x-ray photoelectron spectroscopy *J. Appl. Phys.* **96** 7675-80
[25] Delheusy M, Stierle A, Kasper N, Kurta R P, Vlad A, Dosch H, Antoine C, Resta A, Lundgren E and Andersen J 2008 X-ray investigation of subsurface interstitial oxygen at Nb/oxide interfaces *Appl. Phys. Lett.* **92** 101911
[26] Tian H 2007 Surface oxide study on solid niobium for superconducting RF accelerators using variable photon energy XPS. In: *SRF Workshop,* (Fermilab, Batavia, IL)
[27] Powers R W and Doyle M V 1959 Diffusion of interstitial solutes in the group V transition metals *J. Appl. Phys.* **30** 514-24
[28] Ciovati G 2006 Improved oxygen diffusion model to explain the effect of low-temperature baking on high field losses in niobium superconducting cavities *Appl. Phys. Lett.* **89** 022507
[29] Casalbuoni S, Knabbe E-A, Kotzler J, Lilje L, Sawilski L v, Schmuser P and Steffen B 2005 Surface superconductivity in niobium for superconducting RF cavities *Nucl. Instrum. Meth. A* **538** 45-64
[30] Proslier T, Zasadzinski J, Cooley L, Pellin M, Norem J, Elam J, Antoine C Z, Rimmer R A and Kneisel P 2009 Tunneling study of SRF cavity-grade niobium *Ieee T. Appl. Supercon.* **19** 1404-8
[31] Proslier T, Zasadzinski J F, Cooley L, Antoine C, Moore J, Norem J, Pellin M and Gray K E 2008 Tunneling study of cavity grade Nb: Possible magnetic scattering at the surface *Appl. Phys. Lett.* **92** 212505
[32] Visentin B, Barthe M F, Moineau V and Desgardin P 2010 Involvement of hydrogen-vacancy complexes in the baking effect of niobium cavities *Phys. Rev. ST Accel. Beams* **13** 052002
[33] Romanenko A and Padamsee H 2010 The role of near-surface dislocations in the high magnetic field performance of superconducting niobium cavities *Supercond. Sci. Tech.* **23** 045008
[34] Kresse G and Furthmuller J 1996 Efficient iterative schemes for ab initio total-energy calculations using a plane-wave basis set *Phys. Rev. B* **54** 11169-86
[35] Kresse G and Hafner J 1993 Abinitio molecular-dynamics for liquid-metals *Phys. Rev. B* **47** 558-61
[36] Perdew J P, Burke K and Ernzerhof M 1996 *Phys. Rev. Lett.* **77** 3865
[37] Kresse G and Joubert D 1999 *Phys. Rev. B* **59** 1758-75
[38] Blöchl P E 1994 *Phys. Rev. B* **50** 17953-79
[39] Monkhorst H J and Pack J D 1976 *Phys. Rev. B* **13** 5188-92

[40] Henkelman G, Arnaldsson A and Jónsson H 2006 *Comput. Mater. Sci.* **36** 254
[41] Sanville E, Kenny S D, Smith R and Henkelman G 2007 *J. Comput. Chem.* **28** 899
[42] Tang W, Sanville E and Henkelman G 2009 *J. Phys. Condens. Mat.* **21** 084204
[43] Huber K P and Herzberg G 1979 *Molecular Spectra and Molecular Structure. IV. Constants of Diatomic Molecules* (New York: Van Nostrand Reinhold Co.)
[44] 1991 *Atomic Defects in Metals* vol 25 (Berlin: Springer-Verlag)
[45] Korhonen T, Puska M J and Nieminen R M 1995 Vacancy-formation energies for fcc and bcc transition metals *Phys. Rev. B* **51** 9526-32
[46] Korzhavyi P A, Abrikosov I A and Johansson B 1999 First-principles calculations of the vacancy formation energy in transition and noble metals *Phys. Rev. B* **59** 11693-703
[47] Singer W, Singer X and Wen H M 2003 *Materiaux & Techniques* **91** 13-8
[48] Cooley L and Champion M 2007 Technical specifications for high RRR grade niobium sheet and rod for use in superconducting cavities. In: *Fermilab Engineering Specification,*
[49] Slater J C 1964 *J. Chem. Phys.* **39**
[50] Baker C and Birnbaum H K 1973 Anelastic studies of hydrogen diffusion in niobium *Acta Metall.* **21** 865-72
[51] Pfeiffer G and Wipf H 1975 The trapping of hydrogen in niobium by nitrogen interstitials *J. Phys. F: Met. Phys.* **6** 167-79
[52] Shirley A I, Hall C K and Prince N J 1983 Trapping of hydrogen by oxygen and nitrogen impurities in niobium, vanadium and tantalum *Acta Metall.* **31** 985-92
[53] Mattas R F and Birnbaum H K 1975 Isotope effects on the motion of O-H clusters in Nb *Acta Metall.* **23** 973-7
[54] Blanter M S 1994 Interaction of dissolved atoms and "hydrogen snoek-type relaxation" in Nb and Ta (computer simulation) *J. Alloy Compd.* **211/212** 45-9
[55] Schiller P and Nijam A 1975 *Phys. Stat. Sol. A* **31** K77
[56] Zapp P E and Birnbaum H K 1980 Solute trapping of hydrogen in niobium - symmetry of the O-H pair *Acta Metall.* **28** 1275-86
[57] Metzgert T H, Schubert U and Peisl J 1985 The trapping of hydrogen at nitrogen in niobium investigated by diffuse X-ray scattering *J. Phys. F: Met. Phys.* **15** 779-97
[58] Yagi E, Hirabayashi K, Murakami Y, Koike S, Higami N, Hayashi T, Takebayashi A, Yoshida T, Sugi C, Sugawar T, Shishido T and Ogiwara K 2008 Site change of hydrogen in Nb due to interaction with oxygen *J. Phys. Soc. Japan* **77** 054802
[59] Magerl A, Rush J J, Rowe J M, Richter D and Wipf H 1983 Local hydrogen vibrations in Nb in the presence of interstitial (N,O) and substitutional (V) impurities *Phys. Rev. B* **27** 927-34
[60] Hanada R 1977 Recovery of H and D quenched to 4.2K in interstitial impurities doped Nb and Ta. In: *Second International Congress on Hydrogen in Metals* (Paris, France)
[61] Huang K F, Granato A V and Birnbaum H K 1985 Ultrasonic relaxation from trapped hydrogen in rapidly cooled niobium *Phys. Rev. B* **32** 2178-83
[62] Igata N, Miyahara K, Ohno K and Hakomori K 1982 Detrapping of nitrogen and oxygen atoms from neutron irradiation induced defects of niobium during post-irradiation annealing *J. Nucl. Mater.* **108 & 109** 234-9
[63] Koike H, Shizuku Y, Yazaki A and Fukai Y 2004 Superabundant vacancy formation in Nb–H alloys; resistometric studies *J. Phys.: Condens. Matter* **16** 1335–49
[64] Manchester F D and Pitre J M 2000 (Materials Park, OH: ASM International)
[65] Hautojärvi P, Huomo H, Puska M and Vehanen A 1985 Vacancy recovery and vacancy-hydrogen interaction in niobium and tantalum studied by positrons *Phys. Rev. B* **32** 4326-31
[66] Wechsler M S and Murty K L 1989 Impurity-defect interactions and radiation hardening and embrittlement in bcc metals *Metall. Trans. A* **20A** 2637-49

[67] Brown B S, Blewitt T H, Scott T L and Klank A C 1974 Low-temperature fast-neutron radiation damage studies in superconducting materials *J. Nucl. Mater.* **52** 215-28